ISSN 0543-5846
METABK 64(1-2) 20-22 (2025)
UDC:669.182:66.04:621.791.057:620.18:620.178.1=11

EFFECT OF THE POST WELD HEAT TREATMENT ON THE MICROSTRUCTURE OF THE UNDERWATER WET WELDING SS400 STEEL

Received – Primljeno: 2024-06-30
Accepted – Prihvaćeno: 2024-08-25
Original Scientific Paper – Izvorni znanstveni rad

The effects of the post weld heat treatment (PWHT) on the microstructure and hardness of the underwater wet welding (UWW) SS400 steel have been evaluated. The UWW was performed using Shielded Metal Arc Welding (SMAW) in water depth of 5.0 m, while PWHT was carried out on underwater welded specimen with temperature of 660 °C for 75 minutes. The result showed that the PWHT caused increasing the grain size of the microstructure and decreasing in hardness.

Keywords: SS400 steel, post weld heat treatment, underwater wet welding, microstructure, hardness

INTRODUCTION

Steel is frequently used in structures submerged in water, such as ships, offshore platforms, and oil and gas pipelines. These structures can sustain damage over time, necessitating repairs using underwater welding techniques. Underwater welding is classified into two types based on water contact: dry and wet underwater welding [1]. Among these, underwater wet welding (UWW) is the most commonly used due to its simplicity, suitability for complex structures, low cost, and minimal preparation time [2].

UWW is performed underwater without any barrier between the water and the welding arc. This exposure to hydrostatic pressure makes the welding arc and droplet transfer process unstable, which degrades the quality of the weld joint [2,3]. Additionally, the rapid cooling rate after welding often leads to the formation of martensitic phases [4-8]. The weld joint is also prone to residual stress [9], which can cause cracking and reduce the structure's load-bearing capacity compared to conventional welding [4].

Stress relief through post-weld heat treatment (PWHT) can improve internal stress uniformity and enhance the material's load-bearing capacity [10]. However, research on PWHT has primarily focused on on-land welding [11-12], leaving limited information on PWHT for underwater weld joints. Therefore, this study aims to investigate the effect of PWHT on the microstructure of UWW joints in low-carbon SS400 steel.

EXPERIMENTAL PROCEDURES

This research utilized an SS400 steel plate measuring 400 x 150 x 4 mm. The welding process employed AWS E6013 electrodes with a diameter of 3,2 mm. Table 1 details the chemical composition of both the SS400 steel and the AWS E6013 filler.

The underwater wet welding was performed at a depth of 5 meters using a butt joint design, as illustrated in Figure 1. The process was carried out with a SMAW KOBEWEL KA-602 machine, with the parameters listed in Table 2. After completing the welding, the joint underwent post-weld heat treatment (PWHT). This involved heating the joint in a furnace to 660 °C, maintaining that temperature for 75 minutes, and then allowing it to cool in open air.

To assess the effects of PWHT, microstructure observation and hardness testing were conducted on the underwater weld specimens, both with and without PWHT. This analysis aimed to evaluate the microstructural changes and variations in weld joint hardness resulting from the heat treatment.

Table 1 **Chemical composition of materials / mas. %**

Element	Materials	
	SS400	E6013
P	0,0018	0,3
C	0,0337	0,1
S	0,0	0,03
Mn	0,288	0,6
Cu	0,013	0,0
Si	0,0	0,28
Cr	0,0273	0,0
Fe	Balance	Balance

Table 2 **Underwater welding parameters**

Welding Process	Manual (SMAW)
Type of Joint	butt Joint
Basic Material	SS400
Filler Metal	Type : AWS E6013
	Diameter : 3,2 mm
Current	Polarity : DC +
	Ampere : 90 A
Voltage	38 V

Triyono (e-mail: triyono74@staff.uns.ac.id), N. Muhayat, S. Yasinta, A. R. Prabowo, Mechanical Engineering Department, Universitas Sebelas Maret, Surakarta, Indonesia, Y. C. N. Saputro, UPTB Solo Technopark Technical Unit on Regional Development Planning Board, Surakarta, Indonesia

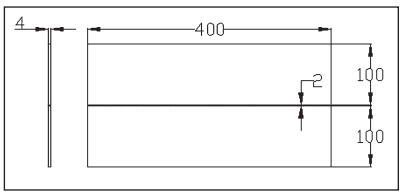

Figure 1 Weld joint configuration / mm

RESULTS AND DISCUSSION

Figure 2 shows the appearance of the beads from underwater and on-land welding. The beads of on-land welding feature smooth grooves and fine weld deposits, with the E6013 electrode producing a smooth bead surface with a fine ripple profile [13]. In contrast, the beads from underwater welding exhibit rough grooves and deposits. This difference is likely due to the varying cooling conditions: on-land welding uses air cooling, whereas underwater welding uses water cooling. Water cooling has a higher cooling rate than air cooling [4-6]. This faster cooling rate affects the material transfer from the electrode to the workpiece, as underwater, the surrounding water hinders the material transfer [8].

Additionally, on-land welding results in a significant amount of spatter, whereas underwater welding produces very little spatter. Spatter refers to the splashing of molten metal from the electrode. During underwater welding, the molten metal splashes from the welding arc solidify quickly upon contact with water, preventing them from reaching the workpiece surface [14].

The welding process causes the weld joint area to experience varying thermal cycles, resulting in different regions: weld metal (WM), heat-affected zone (HAZ), and base metal, each with distinct microstructural morphologies. The microstructure phases observed in the weld metal (WM) are shown in Figure 3. Generally, on-land weld metal, both with and without PWHT, exhibits a microstructure with phases of polygonal ferrite (PF), grain boundary ferrite (GBF), and ferrite with second phase (FSP). Underwater weld metal, both with and without PWHT, shows the same microstructure phases as on-land weld metal but also includes the presence of acicular ferrite (AF).

The increased cooling rate is the primary factor leading to the formation of acicular ferrite (AF) during solidification [6-7]. The ferrite phase transformation mechanism starts in the temperature range of 1530 - 850 °C, where δ-ferrite begins to form and transforms into austenite until the austenite is fully developed. When the temperature reaches the range of 850 - 680 °C, proeutectoid ferrite forms at the austenite grain boundaries. Proeutectoid ferrite consists of GBF, which forms along the austenite grain boundaries during the austenite-to-ferrite transformation, and PF, which grows as coarse ferrite within the austenite grains. In the temperature range of 700 - 550 °C, FSP grows in the austenite region and extends into the interior of the austenite grains that do not fully transform due to prolonged carbon atom diffusion. At around 500 °C, AF grows on inclusions located within the austenite grains, forming needle-like structures [15]. AF only forms if the cooling rate is sufficiently high; otherwise, the phase that forms is pearlite. AF has excellent strength and toughness, making it a beneficial microstructure [16].

The microstructure of WM on-land welds, both without PWHT and with PWHT, as shown in Figures 3 (a) and (b), exhibit almost identical morphologies. Similarly, the microstructures of underwater weld WM, both without PWHT and with PWHT, shown in Figures 3 (c) and (d), are also nearly identical. The noticeable difference is that the grain size in the microstructure of WM with PWHT is larger than that of WM without PWHT. This is due to the heating at 660 °C for 75 minutes during the PWHT process. Although this temperature is below the ferrite-austenite phase transformation temperature, the extended duration allows carbon atoms to diffuse and form a more stable microstructure, with carbon atoms congregating at the grain boundaries, resulting in larger ferrite grains (the light-colored areas). Additionally, PWHT at this temperature is known for stress relief, where residual stresses from the welding process are relieved as the material undergoes stress relaxation.

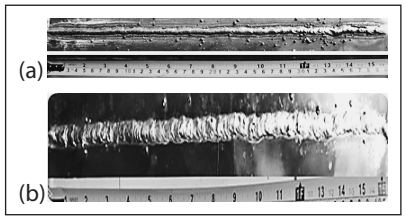

Figure 2 Bead appearance: (a) on-land welding, (b) underwater welding

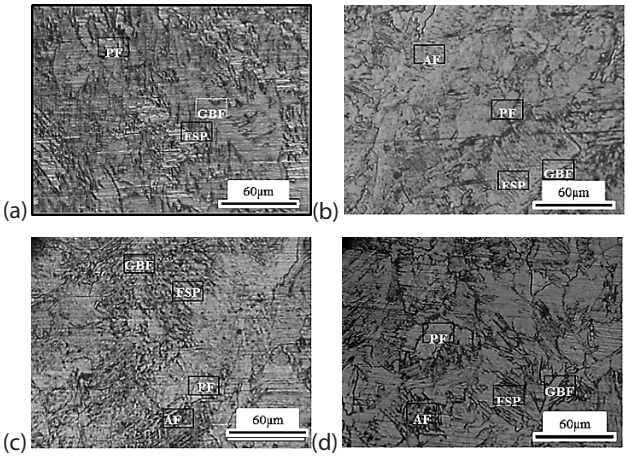

Figure 3 Microstructure of weld metal: (a) on-land without PWHT, (b) on-land with PWHT, (c) underwater without PWHT, and (d) underwater with PWHT

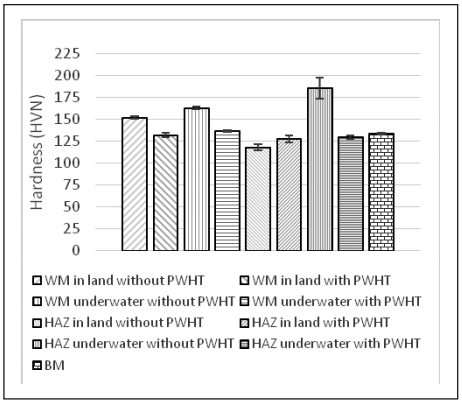

Figure 4 Average hardness in the area of base metal, HAZ, and weld metal

The micro Vickers hardness test results for the base metal (BM), heat-affected zone (HAZ), and weld metal (WM) of both on-land and underwater welding specimens, with and without PWHT, are depicted in Figure 4. The base metal of SS400 steel has a hardness of approximately 130 HVN. This hardness increases in the weld metal of both on-land and underwater welds. Notably, the increase in hardness is more pronounced in underwater weld specimens compared to on-land weld specimens. Interestingly, the hardness of the heat-affected zone (HAZ) is typically lower than that of the base metal, except for the HAZ of underwater weld specimens, which exhibits the highest hardness at 186 HVN. This phenomenon is attributed to the higher cooling rate in underwater welding, driven by forced convection heat transfer when the weld metal and HAZ directly contact water. With a faster cooling rate, the emergence of AF and FSP phases significantly contributes to the heightened hardness of underwater weld specimens.

The average hardness of both the weld metal (WM) and heat-affected zone (HAZ) in both on-land and underwater welds decreases with the PWHT process. PWHT, also known as stress relief, involves reheating the specimen to a temperature of 660 °C and holding it for 75 minutes. During this process, atoms absorb heat energy, allowing them to either move forward or form a greater number of crystals that are freer from stress defects [17]. Areas of the weld joint with high hardness are prone to residual stress, and the decrease in hardness due to PWHT can indicate a reduction in residual stress. Additionally, with PWHT, carbon atoms diffuse to grain boundaries, resulting in the production of ferrite phases with larger grain sizes [17].

CONCLUSIONS

This study shows that underwater weld metal has a higher presence of acicular ferrite (AF) compared to on-land weld metal due to the faster cooling rate. With PWHT at 660 °C for 75 minutes, the microstructure remains unchanged in terms of phases, but the ferrite area increases. PWHT decreases the hardness of weld metal (WM), heat-affected zone (HAZ), and base metal (BM) in both on-land and underwater weld specimens.

ACKNOWLEDGMENTS

The authors are grateful to Universitas Sebelas Maret Surakarta for financing this research through Mandatory Research Grant 2022, with contract no. 254/UN27.22/PT.01.03/2022.

REFERENCES

[1] Y. Fu, and N. Guo, Effect of metal transfer mode on spatter and arc stability in underwater flux-cored wire wet welding, Journal of Manufacturing Processes, 35 (2018), 2, 161-168, doi: 10.1016/j.jmapro.2018.07.027.

[2] H. Chen, N. Guo, X. Zhang, Effect of water flow on the microstructure , mechanical performance and cracking susceptibility of underwater wet welded Q235 and E40 steel, Journal of Materials Processing Tech., 277 (2020), 2, 116435, doi: 10.1016/j.jmatprotec.2019.116435.

[3] Y. Han, S. Dong, M. Zhang, C. Jia, M. Zhang, C. Wu, A novel underwater submerged-arc welding acquires sound quality joints for high strength marine steel, Materials Letters, 261 (2020) 127075. doi: 10.1016/j.matlet.2019.127075.

[4] N. Muhayat, Y. A. Matien, H. Sukanto, Y.C.N. Saputro, Triyono, Fatigue life of underwater wet welded low carbon steel SS400, Heliyon, 6 (2020) e03366 https://doi.org/10.1016/j.heliyon.2020.e03366.

[5] E. Surojo, R. P. Aji, T. Triyono, E. P. Budiana and A. R. Prabowo, Mechanical and Microstructural Properties of A36 Marine Steel Subjected to Underwater Wet Welding, Metals, 11 (2021), 1-15, https://doi.org/10.3390/met11070999.

[6] E. Surojo, A. H. Gumilang, T. Triyono, A. R. Prabowo, E. P. Budiana, N. Muhayat, Effect of Water Flow on Underwater Wet Welded A36 Steel, Metals, 11 (2021), 1-18, https://doi.org/10.3390/met11050682.

[7] E. Surojo, J. Anindito, F. Paundra, A. R. Prabowo, E. P. Budiana, N. Muhayat, M. Badaruddin and Triyono, Effect of water flow and depth on fatigue crack growth rate of underwater wet welded low carbon steel SS400, Open Engineering, 11 (2021), 329-338 https://doi.org/10.1515/eng-2021-0036.

[8] E. Surojo, N. I. Wicaksana, Y. C. N. Saputro, E. P. Budiana, N. Muhayat, Triyono and A. R. Prabowo, Effect of Welding Parameter on the Corrosion Rate of Underwater Wet Welded SS400 Low Carbon Steel, Applied Sciences (Switzerland), 10 (2020), 1–19, https://doi.org/10.3390/app10175843.

[9] M. Phyo, H. Katsuda, and M. Hirohata, Fatigue-performance improvement of patch-plate welding via PWHT with induction heating, Journal of Constructional Steel Research, 160 (2019) 280-288. https://doi.org/10.1016/j.jcsr.2019.05.047

[10] Y. Zhang, C. Jia, B. Zhao, J. Hu, C. Wu, Heat input and metal transfer influences on the weld geometry and microstructure during underwater wet FCAW, Journal of Materials Processing Technology, 238 (2016) 373-382. http://dx.doi.org/10.1016/j.jmatprotec.2016.07.024.

[11] S. S. M. Tavares, M.L. Laurya, H. N. Farneze, R. V. Landim, J. A. C. Velasco, J. L. M. Andia, Influence of PWHT on the sulfide stress cracking susceptibility of 9%Ni low carbon steel, Engineering Failure Analysis, 104 (2019) 331-340 https://doi.org/10.1016/j.engfailanal.2019.05.017.

[12] A. C. Gonzaga, C. Barbosa, S. S. M. Tavares, A. Zeemann, J. C. Payão, Influence of post welding heat treatments on sensitization of AISI 347 stainless steel welded joints, Journal of Materials Research and Technology, 9 (2020), 1, 908-921. https://doi.org/10.1016/j.jmrt.2019.11.031.

[13] A. Rezaeian, M. Keshavarz, E. Hajjari, Mechanical properties of steel welds at elevated temperatures, Journal of Constructional Steel Research, 167 (2020), 105853 https://doi.org/10.1016/j.jcsr.2019.105853.

[14] C. Xu, N. Guo, X. Zhang, H. Chen, Y. Fu, L. Zhou, Internal characteristic of droplet and its influence on the underwater wet welding process stability, Journal of Materials Processing and Technology, 280 (2020), 116593 https://doi.org/10.1016/j.jmatprotec.2020.116593.

[15] C. Wang, X. Wang, J. Kang, G. Yuan and G. Wang, Effect of Thermomechanical Treatment on Acicular Ferrite Formation in Ti–Ca Deoxidized Low Carbon Steel, Metals, 9 (2019), 296. http://dx.doi.org/10.3390/met9030296.

[16] X. Di, S. Ji, F. Cheng, D. Wang, J. Cao, Effect of cooling rate on microstructure, inclusions and mechanical properties of weld metal in simulated local dry underwater welding, Materials and Design, 88 (2015) 505-513. http://dx.doi.org/10.1016/j.matdes.2015.09.025

[17] J. H. An, J. Lee, Y. S. Kim, W. C. Kim, J.G. Kim, Effects of Post Weld Heat Treatment on Mechanical and Electrochemical Properties of Welded Carbon Steel Pipe, Metals and Materials International, 25 (2019), 304-312. https://doi.org/10.1007/s12540-018-0201-9

Note: The responsible English translator is the Native Proofreading Service - in Indonesia.